Beam-Energy Dependence of Charge Separation Along the Magnetic Field in Au + Au Collisions at RHIC

Beam-Energy Dependence of Charge Separation along the Magnetic Field in Au + Au Collisions at RHIC

L. Adamczyk,[1] J. K. Adkins,[23] G. Agakishiev,[21] M. M. Aggarwal,[35] Z. Ahammed,[53] I. Alekseev,[19] J. Alford,[22] C. D. Anson,[32] A. Aparin,[21] D. Arkhipkin,[4] E. C. Aschenauer,[4] G. S. Averichev,[21] A. Banerjee,[53] D. R. Beavis,[4] R. Bellwied,[49] A. Bhasin,[20] A. K. Bhati,[35] P. Bhattarai,[48] H. Bichsel,[55] J. Bielcik,[13] J. Bielcikova,[14] L. C. Bland,[4] I. G. Bordyuzhin,[19] W. Borowski,[45] J. Bouchet,[22] A. V. Brandin,[30] S. G. Brovko,[6] S. Bültmann,[33] I. Bunzarov,[21] T. P. Burton,[4] J. Butterworth,[41] H. Caines,[57] M. Calderón de la Barca Sánchez,[6] D. Cebra,[6] R. Cendejas,[36] M. C. Cervantes,[47] P. Chaloupka,[13] Z. Chang,[47] S. Chattopadhyay,[53] H. F. Chen,[42] J. H. Chen,[44] L. Chen,[9] J. Cheng,[50] M. Cherney,[12] A. Chikanian,[57] W. Christie,[4] J. Chwastowski,[11] M. J. M. Codrington,[48] G. Contin,[26] J. G. Cramer,[55] H. J. Crawford,[5] X. Cui,[42] S. Das,[16] A. Davila Leyva,[48] L. C. De Silva,[12] R. R. Debbe,[4] T. G. Dedovich,[21] J. Deng,[43] A. A. Derevschikov,[37] R. Derradi de Souza,[8] S. Dhamija,[18] B. di Ruzza,[4] L. Didenko,[4] C. Dilks,[36] F. Ding,[6] P. Djawotho,[47] X. Dong,[26] J. L. Drachenberg,[52] J. E. Draper,[6] C. M. Du,[25] L. E. Dunkelberger,[7] J. C. Dunlop,[4] L. G. Efimov,[21] J. Engelage,[5] K. S. Engle,[51] G. Eppley,[41] L. Eun,[26] O. Evdokimov,[10] O. Eyser,[4] R. Fatemi,[23] S. Fazio,[4] J. Fedorisin,[21] P. Filip,[21] E. Finch,[57] Y. Fisyak,[4] C. E. Flores,[6] C. A. Gagliardi,[47] D. R. Gangadharan,[32] D. Garand,[38] F. Geurts,[41] A. Gibson,[52] M. Girard,[54] S. Gliske,[2] L. Greiner,[26] D. Grosnick,[52] D. S. Gunarathne,[46] Y. Guo,[42] A. Gupta,[20] S. Gupta,[20] W. Guryn,[4] B. Haag,[6] A. Hamed,[47] L.-X. Han,[44] R. Haque,[31] J. W. Harris,[57] S. Heppelmann,[36] A. Hirsch,[38] G. W. Hoffmann,[48] D. J. Hofman,[10] S. Horvat,[57] B. Huang,[4] H. Z. Huang,[7] X. Huang,[50] P. Huck,[9] T. J. Humanic,[32] G. Igo,[7] W. W. Jacobs,[18] H. Jang,[24] E. G. Judd,[5] S. Kabana,[45] D. Kalinkin,[19] K. Kang,[50] K. Kauder,[10] H. W. Ke,[4] D. Keane,[22] A. Kechechyan,[21] A. Kesich,[6] Z. H. Khan,[10] D. P. Kikola,[54] I. Kisel,[15] A. Kisiel,[54] D. D. Koetke,[52] T. Kollegger,[15] J. Konzer,[38] I. Koralt,[33] L. Kotchenda,[30] A. F. Kraishan,[46] P. Kravtsov,[30] K. Krueger,[2] I. Kulakov,[15] L. Kumar,[31] R. A. Kycia,[11] M. A. C. Lamont,[4] J. M. Landgraf,[4] K. D. Landry,[7] J. Lauret,[4] A. Lebedev,[4] R. Lednicky,[21] J. H. Lee,[4] M. J. LeVine,[4] C. Li,[42] W. Li,[44] X. Li,[38] X. Li,[46] Y. Li,[50] Z. M. Li,[9] M. A. Lisa,[32] F. Liu,[9] T. Ljubicic,[4] W. J. Llope,[41] M. Lomnitz,[22] R. S. Longacre,[4] X. Luo,[9] G. L. Ma,[44] Y. G. Ma,[44] D. M. M. D. Madagodagettige Don,[12] D. P. Mahapatra,[16] R. Majka,[57] S. Margetis,[22] C. Markert,[48] H. Masui,[26] H. S. Matis,[26] D. McDonald,[49] T. S. McShane,[12] N. G. Minaev,[37] S. Mioduszewski,[47] B. Mohanty,[31] M. M. Mondal,[47] D. A. Morozov,[37] M. K. Mustafa,[26] B. K. Nandi,[17] Md. Nasim,[31] T. K. Nayak,[53] J. M. Nelson,[3] G. Nigmatkulov,[30] L. V. Nogach,[37] S. Y. Noh,[24] J. Novak,[29] S. B. Nurushev,[37] G. Odyniec,[26] A. Ogawa,[4] K. Oh,[39] A. Ohlson,[57] V. Okorokov,[30] E. W. Oldag,[48] D. L. Olvitt, Jr.,[46] M. Pachr,[13] B. S. Page,[18] S. K. Pal,[53] Y. X. Pan,[7] Y. Pandit,[10] Y. Panebratsev,[21] T. Pawlak,[54] B. Pawlik,[34] H. Pei,[9] C. Perkins,[5] W. Peryt,[54] P. Pile,[4] M. Planinic,[58] J. Pluta,[54] N. Poljak,[58] J. Porter,[26] A. M. Poskanzer,[26] N. K. Pruthi,[35] M. Przybycien,[1] P. R. Pujahari,[17] J. Putschke,[56] H. Qiu,[26] A. Quintero,[22] S. Ramachandran,[23] R. Raniwala,[40] S. Raniwala,[40] R. L. Ray,[48] C. K. Riley,[57] H. G. Ritter,[26] J. B. Roberts,[41] O. V. Rogachevskiy,[21] J. L. Romero,[6] J. F. Ross,[12] A. Roy,[53] L. Ruan,[4] J. Rusnak,[14] O. Rusnakova,[13] N. R. Sahoo,[47] P. K. Sahu,[16] I. Sakrejda,[26] S. Salur,[26] J. Sandweiss,[57] E. Sangaline,[6] A. Sarkar,[17] J. Schambach,[48] R. P. Scharenberg,[38] A. M. Schmah,[26] W. B. Schmidke,[4] N. Schmitz,[28] J. Seger,[12] P. Seyboth,[28] N. Shah,[7] E. Shahaliev,[21] P. V. Shanmuganathan,[22] M. Shao,[42] B. Sharma,[35] W. Q. Shen,[44] S. S. Shi,[26] Q. Y. Shou,[44] E. P. Sichtermann,[26] R. N. Singaraju,[53] M. J. Skoby,[18] D. Smirnov,[4] N. Smirnov,[57] D. Solanki,[40] P. Sorensen,[4] H. M. Spinka,[2] B. Srivastava,[38] T. D. S. Stanislaus,[52] J. R. Stevens,[27] R. Stock,[15] M. Strikhanov,[30] B. Stringfellow,[38] M. Sumbera,[14] X. Sun,[26] X. M. Sun,[26] Y. Sun,[42] Z. Sun,[25] B. Surrow,[46] D. N. Svirida,[19] T. J. M. Symons,[26] M. A. Szelezniak,[26] J. Takahashi,[8] A. H. Tang,[4] Z. Tang,[42] T. Tarnowsky,[29] J. H. Thomas,[26] A. R. Timmins,[49] D. Tlusty,[14] M. Tokarev,[21] S. Trentalange,[7] R. E. Tribble,[47] P. Tribedy,[53] B. A. Trzeciak,[13] O. D. Tsai,[7] J. Turnau,[34] T. Ullrich,[4] D. G. Underwood,[2] G. Van Buren,[4] G. van Nieuwenhuizen,[27] M. Vandenbroucke,[46] J. A. Vanfossen, Jr.,[22] R. Varma,[17] G. M. S. Vasconcelos,[8] A. N. Vasiliev,[37] R. Vertesi,[14] F. Videbæk,[4] Y. P. Viyogi,[53] S. Vokal,[21] S. A. Voloshin,[56] A. Vossen,[18] M. Wada,[48] F. Wang,[38] G. Wang,[7] H. Wang,[4] J. S. Wang,[25] X. L. Wang,[42] Y. Wang,[50] Y. Wang,[10] G. Webb,[23] J. C. Webb,[4] G. D. Westfall,[29] H. Wieman,[26] S. W. Wissink,[18] R. Witt,[51] Y. F. Wu,[9] Z. Xiao,[50] W. Xie,[38] K. Xin,[41] H. Xu,[25] J. Xu,[9] N. Xu,[26] Q. H. Xu,[43] Y. Xu,[42] Z. Xu,[4] W. Yan,[50] C. Yang,[42] Y. Yang,[25] Y. Yang,[9] Z. Ye,[10] P. Yepes,[41] L. Yi,[38] K. Yip,[4] I.-K. Yoo,[39] N. Yu,[9] Y. Zawisza,[42] H. Zbroszczyk,[54] W. Zha,[42] J. B. Zhang,[9] J. L. Zhang,[43] S. Zhang,[44] X. P. Zhang,[50] Y. Zhang,[42] Z. P. Zhang,[42] F. Zhao,[7] J. Zhao,[9] C. Zhong,[44] X. Zhu,[50] Y. H. Zhu,[44] Y. Zoulkarneeva,[21] and M. Zyzak[15]

(STAR Collaboration)

[1]AGH University of Science and Technology, Cracow 30-059, Poland
[2]Argonne National Laboratory, Argonne, Illinois 60439, USA
[3]University of Birmingham, Birmingham B15 2TT, United Kingdom
[4]Brookhaven National Laboratory, Upton, New York 11973, USA
[5]University of California, Berkeley, California 94720, USA
[6]University of California, Davis, California 95616, USA
[7]University of California, Los Angeles, California 90095, USA
[8]Universidade Estadual de Campinas, Sao Paulo 13131, Brazil
[9]Central China Normal University (HZNU), Wuhan 430079, China
[10]University of Illinois at Chicago, Chicago, Illinois 60607, USA
[11]Cracow University of Technology, Cracow 31-155, Poland
[12]Creighton University, Omaha, Nebraska 68178, USA
[13]Czech Technical University in Prague, FNSPE, Prague 115 19, Czech Republic
[14]Nuclear Physics Institute AS CR, 250 68 Řež/Prague, Czech Republic
[15]Frankfurt Institute for Advanced Studies FIAS, Frankfurt 60438, Germany
[16]Institute of Physics, Bhubaneswar 751005, India
[17]Indian Institute of Technology, Mumbai 400076, India
[18]Indiana University, Bloomington, Indiana 47408, USA
[19]Alikhanov Institute for Theoretical and Experimental Physics, Moscow 117218, Russia
[20]University of Jammu, Jammu 180001, India
[21]Joint Institute for Nuclear Research, Dubna 141 980, Russia
[22]Kent State University, Kent, Ohio 44242, USA
[23]University of Kentucky, Lexington, Kentucky 40506-0055, USA
[24]Korea Institute of Science and Technology Information, Daejeon 305-701, Korea
[25]Institute of Modern Physics, Lanzhou 730000, China
[26]Lawrence Berkeley National Laboratory, Berkeley, California 94720, USA
[27]Massachusetts Institute of Technology, Cambridge, Massachusetts 02139-4307, USA
[28]Max-Planck-Institut für Physik, Munich 80805, Germany
[29]Michigan State University, East Lansing, Michigan 48824, USA
[30]Moscow Engineering Physics Institute, Moscow 115409, Russia
[31]National Institute of Science Education and Research, Bhubaneswar 751005, India
[32]Ohio State University, Columbus, Ohio 43210, USA
[33]Old Dominion University, Norfolk, Virginia 23529, USA
[34]Institute of Nuclear Physics PAN, Cracow 31-342, Poland
[35]Panjab University, Chandigarh 160014, India
[36]Pennsylvania State University, University Park, Pennsylvania 16802, USA
[37]Institute of High Energy Physics, Protvino 142281, Russia
[38]Purdue University, West Lafayette, Indiana 47907, USA
[39]Pusan National University, Pusan 609735, Korea
[40]University of Rajasthan, Jaipur 302004, India
[41]Rice University, Houston, Texas 77251, USA
[42]University of Science and Technology of China, Hefei 230026, China
[43]Shandong University, Jinan, Shandong 250100, China
[44]Shanghai Institute of Applied Physics, Shanghai 201800, China
[45]SUBATECH, Nantes 44307, France
[46]Temple University, Philadelphia, Pennsylvania 19122, USA
[47]Texas A&M University, College Station, Texas 77843, USA
[48]University of Texas, Austin, Texas 78712, USA
[49]University of Houston, Houston, Texas 77204, USA
[50]Tsinghua University, Beijing 100084, China
[51]United States Naval Academy, Annapolis, Maryland 21402, USA
[52]Valparaiso University, Valparaiso, Indiana 46383, USA
[53]Variable Energy Cyclotron Centre, Kolkata 700064, India
[54]Warsaw University of Technology, Warsaw 00-661, Poland
[55]University of Washington, Seattle, Washington 98195, USA
[56]Wayne State University, Detroit, Michigan 48201, USA
[57]Yale University, New Haven, Connecticut 06520, USA
[58]University of Zagreb, Zagreb HR-10002, Croatia
(Received 5 April 2014; published 30 July 2014)

Local parity-odd domains are theorized to form inside a quark-gluon plasma which has been produced in high-energy heavy-ion collisions. The local parity-odd domains manifest themselves as charge separation along the magnetic field axis via the chiral magnetic effect. The experimental observation of charge separation has previously been reported for heavy-ion collisions at the top RHIC energies. In this Letter, we present the results of the beam-energy dependence of the charge correlations in Au + Au collisions at midrapidity for center-of-mass energies of 7.7, 11.5, 19.6, 27, 39, and 62.4 GeV from the STAR experiment. After background subtraction, the signal gradually reduces with decreased beam energy and tends to vanish by 7.7 GeV. This implies the dominance of hadronic interactions over partonic ones at lower collision energies.

DOI: 10.1103/PhysRevLett.113.052302 PACS numbers: 25.75.-q

A strong interaction is parity even at vanishing temperature and isospin density [1], but parity could be violated locally in microscopic domains in QCD at finite temperature as a consequence of topologically nontrivial configurations of gauge fields [2,3]. The Relativistic Heavy Ion Collider (RHIC) provides a good opportunity to study such parity-odd ($\mathcal{P}$-odd) domains, where the local imbalance of chirality results from the interplay of these topological configurations with the hot, dense, and deconfined quark-gluon plasma created in heavy-ion collisions.

The $\mathcal{P}$-odd domains can be manifested via the chiral magnetic effect (CME). In heavy-ion collisions, energetic protons (mostly spectators) produce a magnetic field (B) with a strength that peaks around $eB \approx 10^4$ MeV^2 [4]. The collision geometry is illustrated in Fig. 1. The strong magnetic field, coupled with the chiral asymmetry in the $\mathcal{P}$-odd domains, induces a separation of electric charge along the direction of the magnetic field [4–9]. Based on data from the STAR [10–13] and PHENIX [14,15] Collaborations at the RHIC and the ALICE Collaboration [16] at the LHC, charge-separation fluctuations have been experimentally observed. The interpretation of these data as an indication of the CME is still under intense discussion; see, e.g., Refs. [13,17,18] and references therein. A study of the beam-energy dependence of the charge-separation effect will shed light on the interpretation of the data.

The magnetic field axis points in the direction that is perpendicular to the reaction plane, which contains the impact parameter and the beam momenta. Experimentally, the charge separation is measured perpendicular to the reaction plane with a three-point correlator $\gamma \equiv \langle \cos(\phi_1 + \phi_2 - 2\Psi_{\mathrm{RP}}) \rangle$ [19]. In Fig. 1, ϕ and Ψ_{RP} denote the azimuthal angles of a particle and the reaction plane, respectively. In practice, we approximate the reaction plane with the "event plane" (Ψ_{EP}) reconstructed with measured particles and then correct the measurement for the finite event plane resolution [10–12].

This Letter reports measurements of the three-point correlator γ for charged particles produced in Au + Au collisions. 8M events were analyzed at the center-of-mass energy $\sqrt{s_{NN}} = 62.4$ GeV (2005), 100M at 39 GeV (2010), 46M at 27 GeV (2011), 20M at 19.6 GeV (2011), 10M at 11.5 GeV (2010), and 4M at 7.7 GeV (2010). Events selected with a minimum bias trigger have been sorted into centrality classes based on uncorrected charged particle multiplicity at midrapidity. Charged particle tracks in this analysis were reconstructed in the STAR time projection chamber [20], within a pseudorapidity range of $|\eta| < 1$ and a transverse momentum range of $0.15 < p_T < 2$ GeV/c. The centrality definition and track quality cuts are the same as in Refs. [21], unless otherwise specified. Only events within 40 cm of the center of the detector along the beam direction were selected for data sets at $\sqrt{s_{NN}} = 19.6$–62.4 GeV. This cut was 50 and 70 cm for 11.5 and 7.7 GeV collisions, respectively. To suppress events from collisions with the beam pipe (radius 3.95 cm), only those events with a radial position of the reconstructed primary vertex within 2 cm were analyzed. A cut on the distance of closest approach to the primary vertex < 2 cm was also applied to reduce the number of weak decay tracks or secondary interactions. The experimental observables involved in the analysis have been corrected for the particle track reconstruction efficiency.

In an event, charge separation along the magnetic field (i.e., perpendicular to the reaction plane) may be described

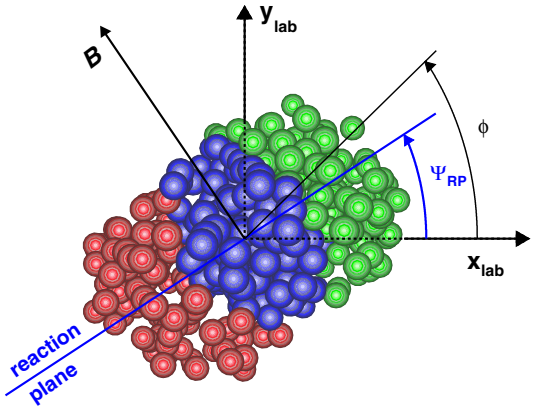

FIG. 1 (color online). Schematic depiction of the transverse plane for a collision of two heavy ions (the left one emerging from and the right one going into the page). Particles are produced in the overlap region (blue-colored nucleons). The azimuthal angles of the reaction plane and a produced particle used in the three-point correlator γ are depicted here.

phenomenologically by a sine term in the Fourier decomposition of the charged particle azimuthal distribution

$$\frac{dN_\alpha}{d\phi} \propto 1 + 2v_1\cos(\Delta\phi) + 2a_\alpha\sin(\Delta\phi) + 2v_2\cos(2\Delta\phi) + \cdots, \quad (1)$$

where $\Delta\phi = \phi - \Psi_{\rm RP}$, and the subscript α (+ or −) denotes the charge sign of particles. Conventionally, v_1 is called "directed flow" and v_2 "elliptic flow," and they describe the collective motion of the produced particles [22]. The parameter a (with $a_- = -a_+$) quantifies the $\mathcal{P}$-violating effect. However, if spontaneous parity violation occurs, the signs of finite a_+ and a_- will vary from event to event, leading to $\langle a_+\rangle = \langle a_-\rangle = 0$. In the expansion of the three-point correlator $\gamma \equiv \langle\cos(\phi_1 + \phi_2 - 2\Psi_{\rm RP})\rangle = \langle\cos(\Delta\phi_1)\cos(\Delta\phi_2) - \sin(\Delta\phi_1)\sin(\Delta\phi_2)\rangle$, the second term contains the fluctuation term $-\langle a_\pm a_\pm\rangle$, which may be nonzero when accumulated over particle pairs of separate charge combinations. The first term ($\langle\cos(\Delta\phi_1)\times\cos(\Delta\phi_2)\rangle$) in the expansion provides a baseline unrelated to the magnetic field.

The reaction plane of a heavy-ion collision is not known *a priori*, and, in practice, it is approximated with an event plane which is reconstructed from particle azimuthal distributions [22]. In this analysis, we exploited the large elliptic flow of charged hadrons produced at midrapidity to construct the event plane angle:

$$\Psi_{\rm EP} = \frac{1}{2}\tan^{-1}\left[\frac{\sum \omega_i \sin(2\phi_i)}{\sum \omega_i \cos(2\phi_i)}\right], \quad (2)$$

where ω_i is a weight for each particle i in the sum [22]. The weight was chosen to be the p_T of the particle itself, and only particles with $p_T < 2$ GeV/c were used. Although the STAR time projection chamber has good azimuthal symmetry, small acceptance effects in the calculation of the event plane azimuth were removed by the method of shifting [23]. The observed correlations were corrected for the event plane resolution which was estimated with the correlation between two random subevents (details are given in Ref. [22]).

The event plane thus obtained from the produced particles is sometimes called "the participant plane" since it is subject to the event-by-event fluctuations of the initial participant nucleons [24]. A better approximation to the reaction plane could be obtained from the spectator neutron distributions detected in the STAR zero degree calorimeters [25]. This type of event plane utilizes the directed flow of spectator neutrons measured at very forward rapidity. We have measured the three-point correlations using both types of reaction plane estimates, and the results are consistent with each other [12]. Other systematic uncertainties were studied extensively and discussed in our previous publications on the subject [10,11]. All were shown to be negligible compared with the uncertainty in determining the reaction plane. In this work, we have only used the participant plane because the efficiency of spectator neutrons detected in the STAR zero degree calorimeters becomes low for low beam energies.

Figure 2 presents the opposite-charge ($\gamma_{\rm OS}$) and same-charge ($\gamma_{\rm SS}$) correlators for Au + Au collisions at $\sqrt{s_{NN}} =$ 7.7–62.4 GeV as a function of centrality (0 means the most central collisions). In most cases, the ordering of $\gamma_{\rm OS}$ and $\gamma_{\rm SS}$ is the same as in Au + Au (Pb + Pb) collisions at higher energies [10–12,16], suggesting charge-separation fluctuations perpendicular to the reaction plane. As a systematic check, the charge combinations of ++ and −− were always found to be consistent with each other (not shown here). With decreased beam energy, both $\gamma_{\rm OS}$ and $\gamma_{\rm SS}$ tend to rise up in peripheral collisions. This feature seems to be charge independent and can be explained by momentum conservation and elliptic flow [12]. Momentum conservation forces all produced particles, regardless of charge, to separate from each other, while elliptic flow, a collective motion, works in the opposite sense. For peripheral collisions, the multiplicity (N) is small, and momentum conservation dominates. At lower beam energies, N also becomes smaller, hence higher values for $\gamma_{\rm OS}$ and $\gamma_{\rm SS}$. For more central collisions where the multiplicity is large, this type of $\mathcal{P}$-even background can be estimated as $-v_2/N$

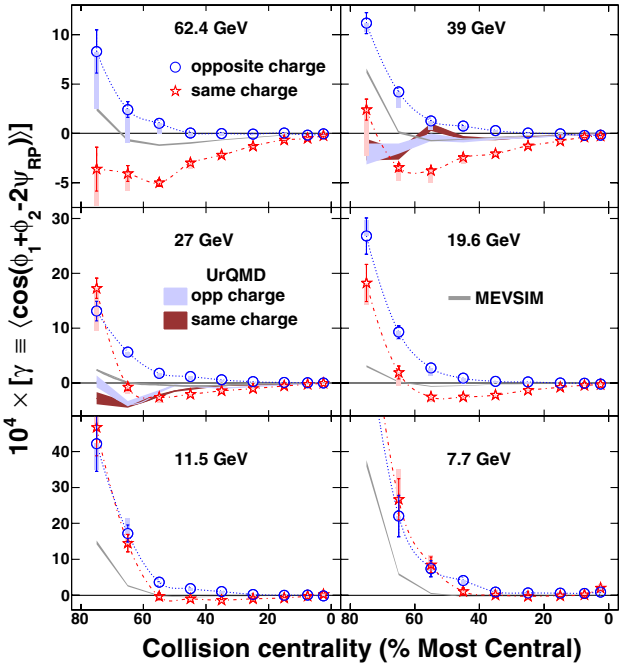

FIG. 2 (color online). The three-point correlator γ as a function of centrality for Au + Au collisions at 7.7–624 GeV. Note that the vertical scales are different for different rows. The filled boxes (starting from the central values) represent one type of systematic uncertainty (as discussed in the text). Charge-independent results from the model calculations of MEVSIM [27] are shown as grey curves. $\gamma_{\rm OS}$ and $\gamma_{\rm SS}$ from UrQMD calculations [28] are also shown as shaded bands for 27 and 39 GeV.

[12,26]. In Fig. 2, we also show the model calculations of MEVSIM, a Monte Carlo event generator with an implementation of v_2 and momentum conservation, developed for STAR simulations [27]. The model results qualitatively describe the beam-energy dependency of the charge-independent background.

In view of the charge-independent background, the charge-separation effect can be studied via the difference between $\gamma_{\rm OS}$ and $\gamma_{\rm SS}$. The difference $(\gamma_{\rm OS} - \gamma_{\rm SS})$ remains positive for all centralities down to the beam energy $\sim$19.6 GeV, and the magnitude decreases from peripheral to central collisions. Presumably, this is partially owing to the reduced magnetic field and partially owing to the more pronounced dilution effect in more central collisions. A dilution of the correlation is expected when there are multiple sources involved in the collision [11,29]. The difference between $\gamma_{\rm OS}$ and $\gamma_{\rm SS}$ approaches 0 in peripheral collisions at lower energies, especially at 7.7 GeV, which could be understood in terms of the CME hypothesis if the formation of the quark-gluon plasma becomes less likely in peripheral collisions at low beam energies [30].

The systematic uncertainties of $(\gamma_{\rm OS} - \gamma_{\rm SS})$ due to the analysis cuts, the track reconstruction efficiency, and the event plane determination were estimated to be approximately 10%, 5%, and 10%, respectively. Overall, total systematic uncertainties are typically 15%, except for the cases where $(\gamma_{\rm OS} - \gamma_{\rm SS})$ is close to 0. Another type of uncertainty is due to quantum interference (HBT effects) and final-state interactions (Coulomb dominated) [12], which are most prominent for low relative momenta. To suppress the contributions from these effects, we applied the conditions of $\Delta p_T > 0.15$ GeV/c and $\Delta\eta > 0.15$ to the correlations, shown as filled boxes in Figs. 2–4. The boxes start from the central values with default conditions and end with the results with the above extra conditions on Δp_T and $\Delta\eta$.

Interpretation of the three-particle correlation result γ requires additional information such as a measurement of the two-particle correlation $\delta \equiv \langle\cos(\phi_1 - \phi_2)\rangle = \langle\cos(\Delta\phi_1)\cos(\Delta\phi_2) + \sin(\Delta\phi_1)\sin(\Delta\phi_2)\rangle$. The expansion of δ also contains the fluctuation term $\langle a_\pm a_\pm\rangle$ (with a sign opposite to that in γ). Figure 3 shows δ as a function of centrality for Au + Au collisions at 7.7–62.4 GeV. Contrary to the CME expectation, $\delta_{\rm OS}$ is above $\delta_{\rm SS}$ in most cases, indicating an overwhelming background, larger than any possible CME effect. The background sources, if coupled with collective flow, will also contribute to γ. Taking this into account, we express γ and δ in the following forms, where the unknown parameter κ, as argued in Ref. [31], is of the order of unity:

$$\gamma \equiv \langle\cos(\phi_1 + \phi_2 - 2\Psi_{\rm RP})\rangle = \kappa v_2 F - H, \quad (3)$$

$$\delta \equiv \langle\cos(\phi_1 - \phi_2)\rangle = F + H, \quad (4)$$

where H and F are the CME and background contributions, respectively. In Ref. [31], $\kappa = 1$, but it could deviate from unity owing to a finite detector acceptance and theoretical uncertainties. We can solve for H from Eqs. (3) and (4):

$$H^\kappa = (\kappa v_2 \delta - \gamma)/(1 + \kappa v_2). \quad (5)$$

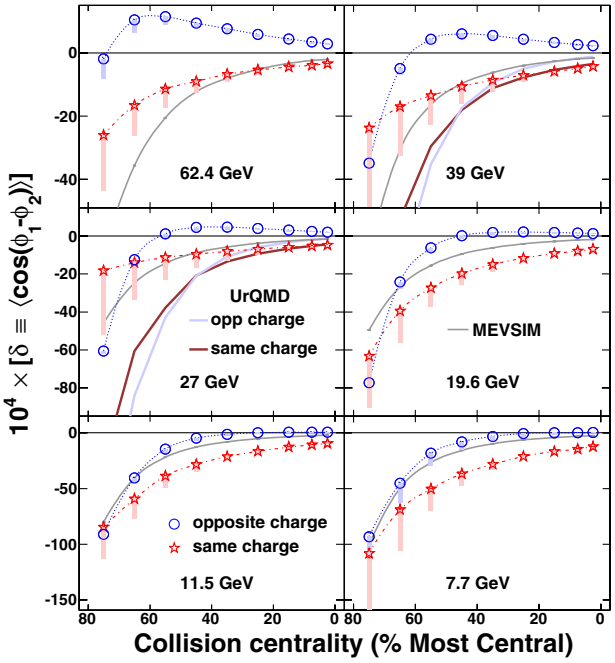

FIG. 3 (color online). The two-particle correlation as a function of centrality for Au + Au collisions at 7.7–62.4 GeV. Note that the vertical scales are different for different rows. The filled boxes bear the same meaning as those in Fig. 2 and are described in the text. MEVSIM and UrQMD calculations are also shown for comparison.

Figure 4 shows $H_{\rm SS} - H_{\rm OS}$ as a function of beam energy for three centrality bins in Au + Au collisions. v_2 for the beam energies under study has been measured in our previous publications [21]. The default values (dotted curves) are for $H^{\kappa=1}$, and the solid (dash-dotted) curves are obtained with $\kappa = 1.5$ ($\kappa = 2$). For comparison, the results for 10%–60% Pb + Pb collisions at 2.76 TeV are also shown [16]. The $(H_{\rm SS} - H_{\rm OS})$ curve for $\kappa = 1$ suggests a nonzero charge-separation effect with a weak energy dependence above 19.6 GeV, but the trend rapidly decreases to 0 in the interval between 19.6 and 7.7 GeV. This may be explained by the probable domination of hadronic interactions over partonic ones at low beam energies. With increased κ, $(H_{\rm SS} - H_{\rm OS})$ decreases for all beam energies and may even totally disappear in some cases (e.g., with $\kappa \sim 2$ in 10%–30% collisions). A better theoretical estimate of κ in the future would enable us to extract a firmer conclusion from the data presented.

MEVSIM calculations qualitatively reproduce the charge-independent background for both γ and δ correlators, as shown in Figs. 2 and 3, but they always yield identical same-charge and opposite-charge correlations. To further

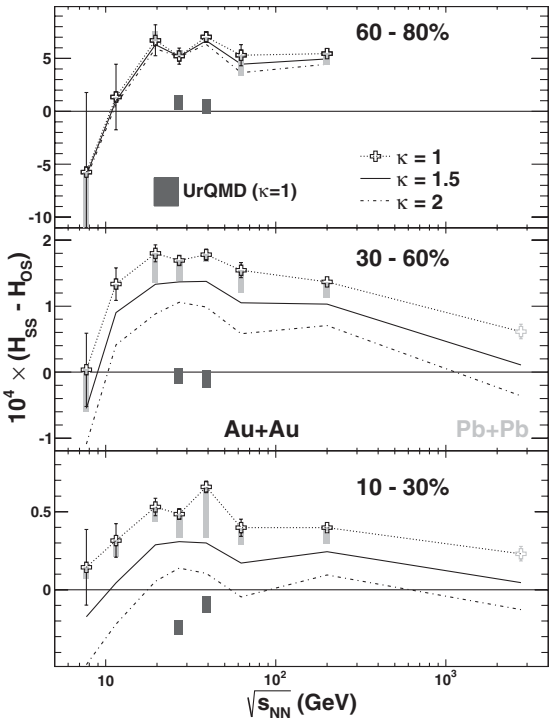

FIG. 4. $H_{SS} - H_{OS}$, as a function of beam energy for three centrality bins in Au + Au collisions. The default values (dotted curves) are for $H^{\kappa=1}$, and the solid (dash-dotted) curves are obtained with $\kappa = 1.5$ ($\kappa = 2$). For comparison, the results for Au + Au collisions at 200 GeV [11] and Pb + Pb collisions at 2.76 TeV [16] are also shown. The systematic errors of the STAR data (filled boxes) bear the same meaning as those in Fig. 2. UrQMD calculations with $\kappa = 1$ are also shown as solid shaded bars for 27 and 39 GeV.

study the charge-separation effect, a transport model UrQMD [28] was employed. UrQMD calculations have finite difference between same-charge and opposite-charge γ (δ) correlations, while $H_{SS} - H_{OS}$ is either slightly negative or consistent with 0. This is demonstrated for 27 and 39 GeV in Figs. 2–4.

In summary, an analysis of the three-point correlation between two charged particles and the reaction plane has been carried out for Au + Au collisions at $\sqrt{s_{NN}} = 7.7$–62.4 GeV. The general trend of the correlations (γ_{OS} and γ_{SS}), as a function of centrality and beam energy, can be qualitatively described by the model calculations of MEVSIM. This result indicates a large contribution from the $\mathcal{P}$-even background due to momentum conservation and collective flow. The charge separation along the magnetic field, studied via ($H_{SS} - H_{OS}$), shows a signal with a weak energy dependence down to 19.6 GeV and then falls steeply at lower energies. This trend may be consistent with the hypothesis of local parity violation because there should be a smaller probability for the CME at lower energies where the hadronic phase plays a more dominant role than the partonic phase. A more definitive result may be obtained in the future if we can increase the statistics by a factor of 10 for the low energies and if we can reduce the uncertainty associated with determination of the value of κ.

We thank the RHIC Operations Group and RCF at BNL, the NERSC Center at LBNL, the KISTI Center in Korea, and the Open Science Grid consortium for providing resources and support. This work was supported in part by the Offices of NP and HEP within the U.S. DOE, Office of Science; the U.S. NSF; CNRS/IN2P3; FAPESP CNPq of Brazil; the Ministry of Education and Science of the Russian Federation; NNSFC, CAS, MoST, and MoE of China; the Korean Research Foundation; GA and MSMT of the Czech Republic; FIAS of Germany; DAE, DST, and CSIR of India; the National Science Centre of Poland; the National Research Foundation (NRF-2012004024); the Ministry of Science, Education and Sports of the Republic of Croatia; and RosAtom of Russia.

[1] C. Vafa and E. Witten, Phys. Rev. Lett. **53**, 535 (1984).
[2] T. D. Lee, Phys. Rev. D **8**, 1226 (1973).
[3] T. D. Lee and G. C. Wick, Phys. Rev. D **9**, 2291 (1974).
[4] D. E. Kharzeev, L. D. McLerran, and H. J. Warringa, Nucl. Phys. **A803**, 227 (2008).
[5] D. Kharzeev, Phys. Lett. B **633**, 260 (2006).
[6] D. Kharzeev and A. Zhitnitsky, Nucl. Phys. **A797**, 67 (2007).
[7] K. Fukushima, D. E. Kharzeev, and H. J. Warringa, Phys. Rev. D **78**, 074033 (2008).
[8] D. E. Kharzeev, Ann. Phys. (Amsterdam) **325**, 205 (2010).
[9] R. Gatto and M. Ruggieri, Phys. Rev. D **85**, 054013 (2012).
[10] B. I. Abelev *et al.* (STAR Collaboration), Phys. Rev. Lett. **103**, 251601 (2009).
[11] B. I. Abelev *et al.* (STAR Collaboration), Phys. Rev. C **81**, 054908 (2010).
[12] L. Adamczyk *et al.* (STAR Collaboration), Phys. Rev. C **88**, 064911 (2013).
[13] L. Adamczyk *et al.* (STAR Collaboration), Phys. Rev. C **89**, 044908 (2014).
[14] N. N. Ajitanand, S. Esumi, and R. A. Lacey (PHENIX Collaboration), in *Proceedings of the RBRC Workshops, 2010*, Vol. 96, http://www.bnl.gov/isd/documents/74466.pdf.
[15] N. N. Ajitanand, R. A. Lacey, A. Taranenko, and J. M. Alexander, Phys. Rev. C **83**, 011901 (2011).
[16] B. I. Abelev *et al.* (ALICE Collaboration), Phys. Rev. Lett. **110**, 012301 (2013).
[17] A. Bzdak, V. Koch, and J. Liao, Phys. Rev. C **81**, 031901 (2010); J. Liao, V. Koch, and A. Bzdak, Phys. Rev. C **82**, 054902 (2010).
[18] D. E. Kharzeev and D. T. Son, Phys. Rev. Lett. **106**, 062301 (2011).
[19] S. A. Voloshin, Phys. Rev. C **70**, 057901 (2004).
[20] M. Anderson *et al.*, Nucl. Instrum. Methods Phys. Res., Sect. A **499**, 659 (2003).
[21] J. Adams *et al.* (STAR Collaboration), Phys. Rev. C **72**, 014904 (2005); G. Agakishiev *et al.* (STAR Collaboration), Phys. Rev. C **86**, 014904 (2012); L. Adamczyk *et al.* (STAR Collaboration), Phys. Rev. C **86**, 054908 (2012).

[22] A. M. Poskanzer and S. A. Voloshin, Phys. Rev. C **58**, 1671 (1998).
[23] J. Barrette *et al.*, Phys. Rev. C **56**, 3254 (1997).
[24] J.-Y. Ollitrault, A. M. Poskanzer, and S. A. Voloshin, Phys. Rev. C **80**, 014904 (2009).
[25] B. I. Abelev *et al.* (STAR Collaboration), Phys. Rev. Lett. **101**, 252301 (2008) and references therein.
[26] A. Bzdak, V. Koch, and J. Liao, Phys. Rev. C **83**, 014905 (2011).
[27] R. L. Ray and R. S. Longacre, arXiv:nucl-ex/0008009; R. L. Ray and R. S. Longacre (private communication).
[28] S. A. Bass *et al.*, Prog. Part. Nucl. Phys. **41**, 255 (1998); M. Bleicher *et al.*, J. Phys. G **25**, 1859 (1999).
[29] G.-L. Ma and B. Zhang, Phys. Lett. B **700**, 39 (2011).
[30] V. A. Okorokov, Int. J. Mod. Phys. E **22**, 1350041 (2013).
[31] A. Bzdak, V. Koch, and J. Liao, Lect. Notes Phys. **871**, 503 (2013).